Regular to chaotic transition of stick–slip motion in sliding friction of an adhesive gel-sheet

2009 J. Phys.: Condens. Matter 21 205105

(http://iopscience.iop.org/0953-8984/21/20/205105)

IOP PUBLISHING JOURNAL OF PHYSICS: CONDENSED MATTER

J. Phys.: Condens. Matter **21** (2009) 205105 (7pp) doi:10.1088/0953-8984/21/20/205105

Regular to chaotic transition of stick–slip motion in sliding friction of an adhesive gel-sheet

Tetsuo Yamaguchi, Satoshi Ohmata and Masao Doi

Department of Applied Physics, University of Tokyo, Tokyo 113-8656, Japan

Received 19 January 2009, in final form 9 March 2009
Published 21 April 2009
Online at stacks.iop.org/JPhysCM/21/205105

Abstract

Spatio-temporal pattern of the stick–slip motion of a gel-sheet pulled on a glass substrate is observed. The sliding takes place via the propagation of the wave of detachment (Schallamach wave). At large pull velocity, the detached region is a stripe which moves regularly with constant speed and the frictional force shows a periodic time dependence. As the pull velocity is decreased, the detached region is separated into bubbles which move around irregularly. In the irregular state, the frictional force shows chaotic time dependence and the statistics of the event of the force drop obeys a power law similar to the Gutenberg–Richter law known in earthquakes. In the regular region, the detachment wave is analyzed theoretically and the velocity and lengths are obtained as a function of the pull velocity. The transition from the regular to chaotic behavior is shown to be related to the spontaneous wetting of the gel.

(Some figures in this article are in colour only in the electronic version)

1. Introduction

The dynamic process of stick–slip motion is important in the sliding friction of soft elastic materials such as rubber and gel on a hard substrate [1–16]. In many situations, the sliding takes place via the propagation of slip regions. A classical example is the Shallamach wave [7–13] which appears when rubber is slid on a smooth substrate. In the Shallamach wave, some regions of the rubber are detached from the substrate and propagate along the interface. This causes the motion of the material relative to the substrate despite the fact that there is no slippage taking place in the contact region. The Schallamach wave has been considered to be the main mechanism of the sliding friction above a certain sliding velocity.

The slip–stick motion of soft matter on a hard substrate has also been studied as a model for earthquake dynamics. Rubio and Galeano [14] studied the slippage of gelatin gel on various hard surfaces (Teflon, plexiglass and stainless steel) and found various types of slip–stick motion: steady slippage, the regular propagation of the slip region and chaotic motion. Baumberger *et al* [15, 16] studied the phenomena in a more systematic way and reported how the slip region moves in time and how it is related to the frictional force and the gel parameters. In their system, the mechanism of slip motion was considered to be different from the Schallamach wave since there is no observable detached region and the slip region heals gradually.

In this paper, we shall report an experimental system which is suited for the study of the spatio-temporal pattern of slip–stick motion. It is an adhesive gel-sheet backed by a plastic film pulled on a glass substrate. In this system, the relative motion takes place via the propagation of the wave of detachment (the Schallamach wave). The advantage of the system is that (i) unlike the classical work of Schallamach (soft rubber slid on a substrate), the geometry is simple and suited for theoretical analysis and (ii) the detached part is visible by a simple setting and is therefore suited for the study of the change of the spatial pattern.

We shall show that this system undergoes a transition from the regular detachment wave motion to an irregular motion of the detached region. The frictional force oscillates periodically in the former case, while it shows chaotic behavior which obeys the power law statistics. We shall conduct a simple analysis for the motion of the regular detachment wave and predict the velocity of the detachment wave as a function of the pull velocity of the gel. We also discuss the condition for the transition from the regular to chaotic motion.

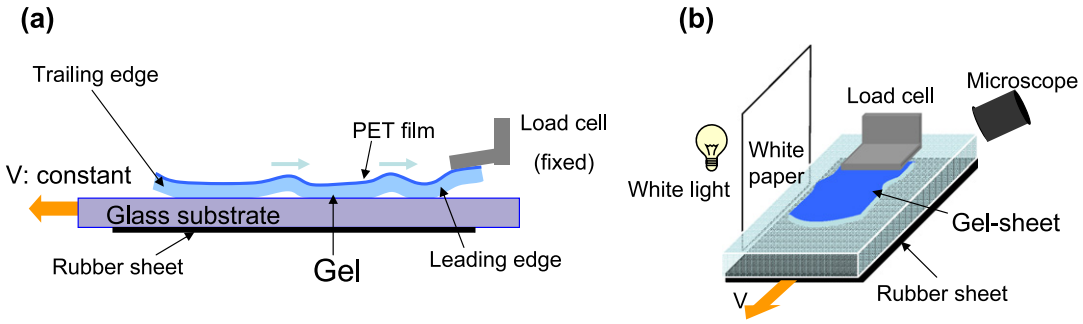

Figure 1. Schematic figures of the experimental apparatus for (a) sliding of an adhesive gel-sheet and (b) visualization of the contact/non-contact regions.

2. Experiment

2.1. Sample

A polyethylene-type adhesive gel-sheet (thickness $H = 5$ mm, commercial name: Super Gel, Kihara Sangyo Co. Ltd, Japan) is cut into a sheet of width $W = 70$ mm and span $L = 150$ mm. A PET film ($t = 50$ μm) was adhered to one side of the gel-sheet in a bent state. As a result, the sample has a spontaneous curvature ($R = 75$ mm) toward the frictional surface. Since the PET film is inextensible, only bending and shearing are allowed for the deformation of the gel. Viscoelasticity of the gel was measured by a rheometer (Haake, parallel plate, $d = 20$ mm) for the frequency range from 0.01 to 10 s^{-1} at 23°. The storage modulus was about 15 kPa for all the range and the loss modulus changed from 0.1 kPa (0.01 s^{-1}) to 1.0 kPa (10 s^{-1}).

2.2. Friction experiment

Figure 1(a) shows the experimental set-up. The right end of the gel-sheet is fixed to the load cell and the left end of the gel-sheet is free. The gel-sheet was placed on a glass substrate, which was driven at a constant velocity V. The frictional force F acting on the gel-sheet was measured by the load cell. The pull velocity was varied from 1000 to 1 μm s^{-1}. During the friction experiments, we observed no solvent coming out from the gel. Therefore the lubrication effect is negligible in our system, unlike the gel systems reported in [15, 16].

2.3. Visualization

The spatial pattern of the detached region was observed as is shown in figure 1(b). To enhance the contrast between the contact region and the non-contact region (i.e. the detached region), a black rubber sheet was adhered onto the bottom side of the glass substrate and the gel-sheet was illuminated by white light. The sliding images were taken by a CCD camera (VHX-200, Keyence, Japan).

3. Results and discussion

3.1. Sliding patterns

Figures 2(a)–(c) are typical snapshots of the gel-sheet at various pull velocities. The dark region stands for the area where the gel-sheet is in contact with the glass substrate and the pale region stands for the area where the gel is lifted above the glass substrate.

At a large pull velocity of $V = 1000$ μm s^{-1} (figure 2(a)), a regular stripe pattern is seen. As the glass plate is pulled relative to the gel-sheet, a non-contact region is generated at the trailing edge of the gel-sheet and propagates towards the leading edge.

At a small velocity of $V = 2$ μm s^{-1} (figure 2 (c)), a bubble-like pattern is seen. Small non-contact domains are generated at the trailing edge and move into the bulk of the sample, which is similar to the bubbles previously reported by Chaudhury *et al* [17]. The difference is that the bubbles wander around in the sample: interestingly, they stop occasionally or even move backwards.

At an intermediate velocity ($V = 50$ μm s^{-1}, figure 2 (b)), the motion becomes transient: the stripe pattern looks unstable and breaks into two or more pieces in the middle of the sample.

While the observed phenomena are similar to those of the Schallamach wave [7–13] in the sense that there is no apparent slippage and the detachment waves propagating via the crack opening and resticking, the underlying mechanism is different from the original one [7]: there is no buckling instability in our system and the crack opening of our system is due to the release of the shear strain energy [18].

3.2. Frictional forces

Figures 3(a)–(c) show the time evolution of the frictional force F for the three cases shown in figure 2. It is seen that the frictional force varies with time: cyclic force oscillations are observed at large pull velocities and, as we decrease the pull velocity, it has wider frequency components. In particular, the drop of the frictional force at smaller pull velocities is reminiscent of the Gutenberg–Richter law for earthquakes [19–21]. This will be discussed in section 3.3.

Figure 4 shows the time-averaged force F_{ave} plotted against the pull velocity V (the error bars are taken for three different trials). In the stripe region, the average force increases with the increase of the pull velocity. On the other hand, in the bubble region, the frictional force is almost constant. In the transient region, there is no definite transition velocity from one region to another and the force had large variations among different trials. Figures 2 and 3 suggest that the system

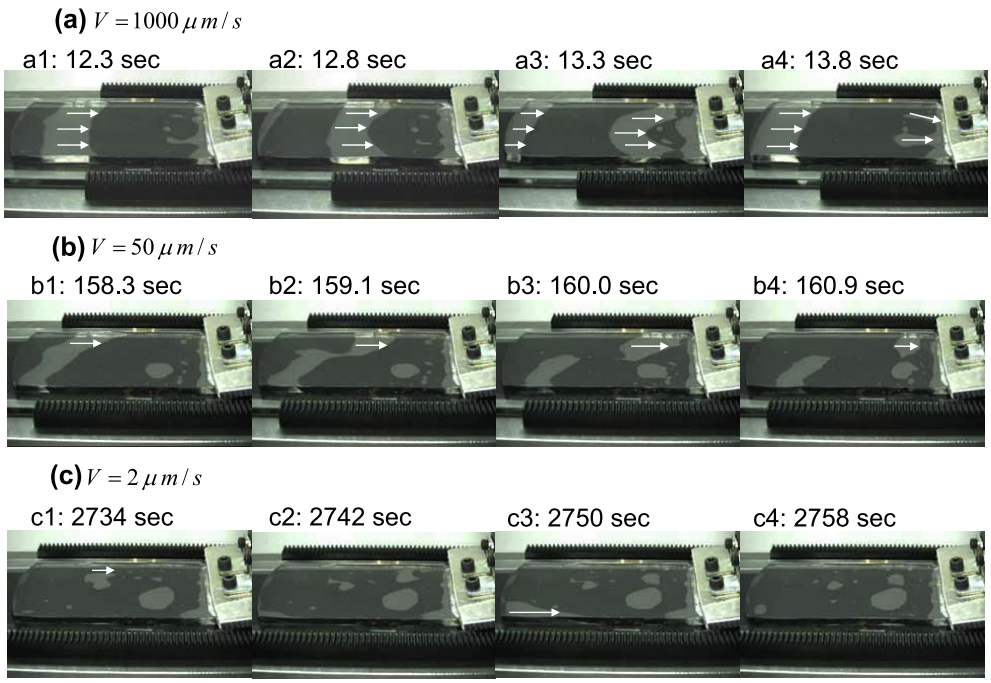

Figure 2. Snapshot of the sliding behavior at pull velocities (a) $V = 1000\ \mu$m s^{-1}, (b) $V = 50\ \mu$m s^{-1} and (c) $V = 2\ \mu$m s^{-1}. Arrows stand for the moving directions of each non-contact region. The time shown in the figures displays the time elapsed since the experiment was started.

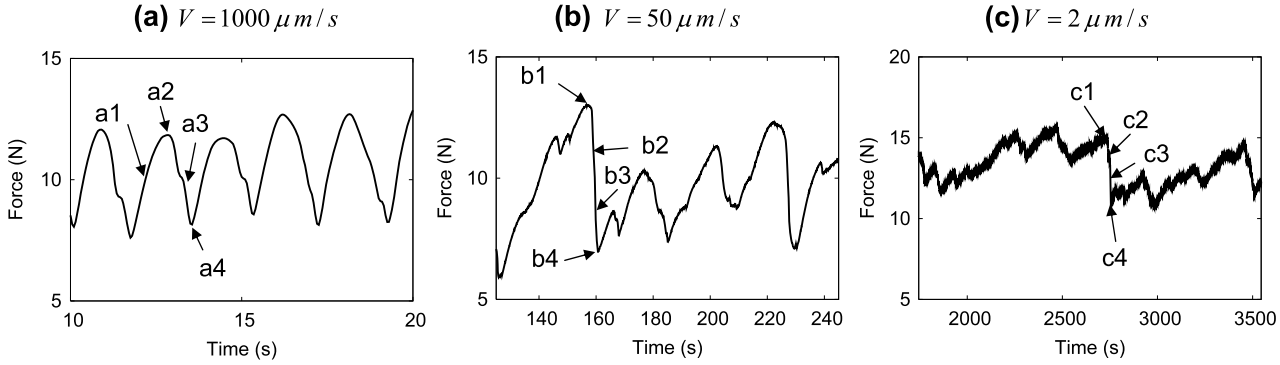

Figure 3. Time–force curves at (a) pull velocity $V = 1000\ \mu$m s^{-1}, (b) $V = 50\ \mu$m s^{-1} and (c) $V = 2\ \mu$m s^{-1}. The points (a1–c4) correspond to the snapshots in figure 2.

undergoes a transition from the stripe (regular) to the bubble (chaotic) state at intermediate pull velocity.

3.3. Size distribution of the force drop

As is seen in figure 3, the frictional force varies irregularly with time. In order to study the statistics for the force variations, we plotted in figure 5(a) the cumulative probability distributions of the force drop ΔF, which is defined by the top-to-bottom force for each force-dropping (energy releasing) event. The force drop corresponds to the earthquake moment in seismology [22, 23] and also to the displacement in granular systems [24, 25]. At large pull velocity, only large events ($\Delta F > 1$ N) are observed. On the other hand, at smaller pull velocity, the force drop obeys a power law distribution, where

$$\log_{10}(\text{Prob}(\text{event} \geqslant \Delta F)) \approx a - b \log_{10}(\Delta F). \qquad (1)$$

Such a power law distribution suggests that the dynamics in the bubble state corresponds to the self-organized criticality [22, 23, 26–28], which has been observed in granular systems [24, 25]. As far as we know, this is the first observation of the SOC state in a homogeneous elastic system. The slope (which is called the b value in seismology) changes from 1.8 ($V = 1\ \mu$m s^{-1}) to almost 0 as we increase the pull velocity, as shown in figure 5(b).

It is important to note here that the removal of the measurement noise is needed to obtain the correct size distributions, since the calculated force drop value is greatly influenced by the measurement noise. In our analysis, we first measured the force without loading and obtained the noise level as 0.05 N. We then 'rounded down' the raw force data by 0.05 N. To check the validity of the noise level, we also analyzed the sensitivity of the rounded-down value to the size

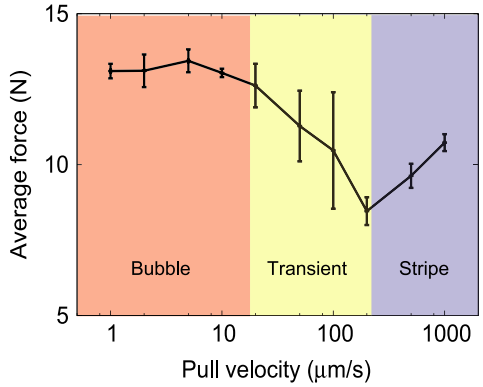

Figure 4. Pull velocity–time averaged friction force curve.

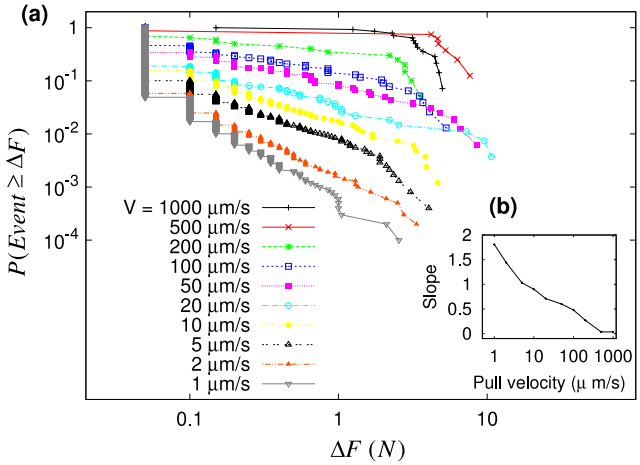

Figure 5. (a) Cumulative probability distributions for the force drop ΔF from $V = 1000$ to 1 μm s^{-1} and (b) the slope (b value) of the straight region for each cumulative distribution in (a). In order to obtain the plots, we rounded down the raw force data by the noise value (0.05 N), which was determined by experiments without loading.

distributions from 0.05 to 0.2 N. The rounded-down value affected the number of events, but did not affect the slopes so much. We finally decided to adopt 0.05 N as the rounded-down value.

3.4. Modeling the frictional behavior at larger pull velocities

We now discuss the frictional behavior of the gel-sheet at large pull velocity, where the sliding is caused by the steady motion of the detached region.

Figure 6(a) shows an idealized configuration of the gel in the steady sliding state. Since the top PET film is inextensible and the bottom substrate is moving with velocity V, a shearing stress is created within a gel. In order to release the shearing energy, a part of the gel is detached from the substrate but sticks again after some time. This creates a non-contact region at the interface between the gel and the substrate. Let L_c and L_n be the length of the contact region and the non-contact region per stripe, respectively.

As the bottom substrate moves, both the contact region and the non-contact region moves rightward with the velocity v. This movement is caused by the detachment of the gel from the substrate at the left end of the contact region and the resticking at the right end of the contact region. We shall call the detaching end the opening crack edge and the resticking end the closing crack edge.

The detachment is a fracture process taking place at the interface between the gel and the substrate. Let G_c be the work needed to decrease the unit area of the contact region: G_c is called the critical energy release rate in fracture mechanics. It is known that G_c is much larger than the thermodynamic surface energy since the detachment of the gel is associated with a large energy dissipation taking place near the crack tip. G_c is a function of the velocity v of the crack tip [29]. We assume the following model for the adhesion hysteresis [8, 9]:

$$G_c(v) = G_0\left(\frac{v}{v_0}\right)^{\alpha}, \tag{2}$$

where G_0 is the thermodynamic work of adhesion, v_0 is the characteristic velocity and α is the exponent. The parameters v_0 and α can be related to the viscoelasticity of the material [29].

We now discuss the shear strain in the gel. We assume that the shear strain is zero at the closing crack edge. Since the substrate moves at velocity V with the detachment wave propagating at velocity v, the attached gel segment separated

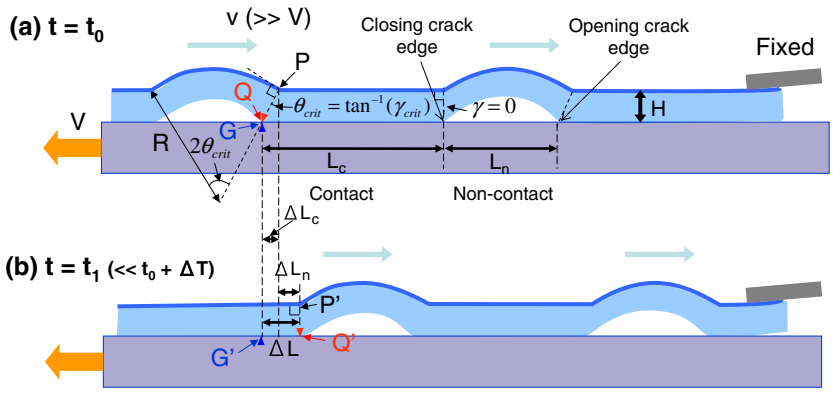

Figure 6. Geometry of our model and snapshots of the deformation of the gel-sheet at (a) $t = t_0$ and (b) $t = t_1$.

from the closing crack by a distance d is sheared by

$$\gamma(d) = \frac{Vt(d)}{H} = \frac{d}{H}\frac{V}{v}, \tag{3}$$

where H is the thickness of the gel and $t(d) = d/v$ is the contact time elapsed since the gel element at d last restuck. From equation (3), the shear strain of the gel increases linearly with the distance from the closing crack edge. Therefore the shear strain is largest when d is equal to L_c (the length of the contact region) and the critical shear strain is given by

$$\gamma_{crit} = \frac{L_c}{H}\frac{V}{v}. \tag{4}$$

Since the gel cannot slip in the region contacting the substrate, the displacement of the gel relative to the substrate is caused by an inchworm-like motion. To evaluate the relative displacement gained by a cycle of the inchworm motion, we consider the situation shown by figure 6(a), where the crack opening has just occurred at the material point Q at the bottom of the gel-sheet. Let G be the material point located at the substrate touching the point Q and P be the material point in the gel which is above the point Q in the natural state. (The line segment PQ would be normal to the substrate if the shearing force of the gel is set to zero.) In figure 6(a), the gel is sheared and therefore PQ makes an angle $\theta_{crit} = \tan^{-1}(\gamma_{crit})$ against the vertical line. After some time, the detachment wave passes through the part PQ and we will have the situation shown in figure 6(b). Here the material points P and Q have moved to point P′ and Q′, respectively. Since the gel is shear free at the moment of resticking, the line segment P′Q′ is now normal to the substrate. Notice that the points P′ and Q′ have moved to the right relative to the points P and Q due to the passage of the detachment wave, while the point G′ has moved little since the pull velocity V is much less than the velocity of the detachment wave v ($V \ll v$).

The relative displacement (effective slip) per wave ΔL consists of two parts:

$$\Delta L = \Delta L_c + \Delta L_n, \tag{5}$$

where ΔL_c is the displacement caused by the release of the shear strain in the contact region and ΔL_n is the displacement caused by the passage of the detachment wave. ΔL_c is given by the critical shear strain γ_{crit}:

$$\Delta L_c = H\gamma_{crit}. \tag{6}$$

On the other hand, ΔL_n is given by the difference between the horizontal distance L_n and the contour distance of the detached part of the gel. As we mentioned in the previous section, our gel-sheet has a spontaneous curvature $1/R$. We assume that the detached part of the gel is a force-free state and therefore has this curvature $1/R$. Furthermore, we assume that the detached sheet is lifted approximately at an angle $\theta_{crit} = \tan^{-1}(\gamma_{crit})$ against the substrate as was discussed by Kendall [30]. (Actually, the radius maybe altered by an applied tension or gravitational force, but this simplification will give a rough estimate for the non-contact length L_n.) With these assumptions, the horizontal distance L_n of the detached part is given by

$$L_n = 2R\sin\theta_{crit}. \tag{7}$$

On the other hand, the contour distance is given by $2R\theta_{crit}$. The difference gives ΔL_n:

$$\Delta L_n = 2R(\theta_{crit} - \sin\theta_{crit}) \approx \frac{R}{3}\theta_{crit}^3 \approx \frac{R}{3}\gamma_{crit}^3. \tag{8}$$

From equations (6) and (8), the total relative displacement per wave (equation (5)) is given by the following equation:

$$\Delta L \approx H\gamma_{crit} + \frac{R}{3}\gamma_{crit}^3. \tag{9}$$

On the other hand, the total relative displacement is also linked with the period of the wave T and the pull velocity V. From equations (4) and (7)

$$\Delta L = VT = V\frac{L_c + L_n}{v} \approx \frac{V}{v}\left(H\frac{v}{V} + 2R\right)\gamma_{crit}. \tag{10}$$

From equations (9) and (10), we obtain the following relation:

$$\gamma_{crit} = \sqrt{6\frac{V}{v}}. \tag{11}$$

Equation (11) is the final result obtained by the geometrical consideration for the steady sliding of the gel-sheet. According to equation (11), the critical strain (the strain at the crack opening edge) decreases with the increase of the crack propagation velocity v. This is because the contact time decreases with the increase of v.

Now let us consider the kinetics. When the gel-sheet is detached from the substrate, an elastic strain energy $G \approx (\mu H/2)\gamma_{crit}^2$ is released per unit area [18], where μ is the shear modulus of the gel. This energy is used to open the crack. If we assume that all the released elastic energy is consumed in the dissipation associated with the crack opening, G is equal to $G_c(v)$ (here we neglect the energy dissipation for the closing crack [29]). The relation $G = G_c(v)$ gives

$$\frac{\mu H}{2}\gamma_{crit}^2 \approx G_0\left(\frac{v}{v_0}\right)^{\alpha}. \tag{12}$$

From equations (11) and (12), we obtain the following results:

$$v = v_0\left(\frac{3\mu H}{G_0}\right)^{\frac{1}{1+\alpha}}\left(\frac{V}{v_0}\right)^{\frac{1}{1+\alpha}}, \tag{13}$$

$$\gamma_{crit} = \sqrt{6}\left(\frac{3\mu H}{G_0}\right)^{-\frac{1}{2(1+\alpha)}}\left(\frac{V}{v_0}\right)^{\frac{\alpha}{2(1+\alpha)}}. \tag{14}$$

Furthermore, from equations (4) and (7)

$$L_c = \sqrt{6}H\left(\frac{3\mu H}{G_0}\right)^{\frac{1}{2(1+\alpha)}}\left(\frac{V}{v_0}\right)^{-\frac{\alpha}{2(1+\alpha)}}, \tag{15}$$

$$L_n = 2\sqrt{6}R\left(\frac{3\mu H}{G_0}\right)^{-\frac{1}{2(1+\alpha)}}\left(\frac{V}{v_0}\right)^{\frac{\alpha}{2(1+\alpha)}}. \tag{16}$$

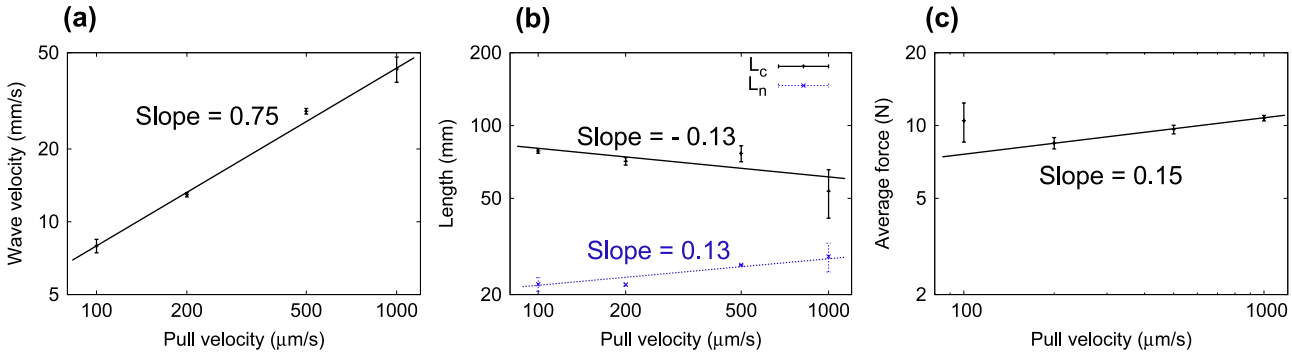

Figure 7. Experimental results for the pull velocity dependence on (a) wave velocity, (b) contact and non-contact length and (c) friction force. The slopes in the figures were determined by the least-squares fitting.

The average force can be also calculated by

$$F_{\rm ave} = \frac{L_{\rm c}}{L_{\rm c}+L_{\rm n}}\frac{\mu\gamma_{\rm crit}}{2}LW \approx \frac{\mu\gamma_{\rm crit}}{2}LW,$$

where L and W are the sample length and width, respectively. From equation (14), we have

$$F_{\rm ave} \approx \frac{\sqrt{6}\mu LW}{2}\left(\frac{G_0}{3\mu H}\right)^{\frac{1}{2(1+\alpha)}}\left(\frac{V}{v_0}\right)^{\frac{\alpha}{2(1+\alpha)}} \qquad (17)$$

which satisfies the energy dissipation relation [8, 9]

$$F_{\rm ave}V = nWG_{\rm c}(v)v, \qquad (18)$$

where $n = L/(L_{\rm c}+L_{\rm n}) \approx L/L_{\rm c}$ is the number of waves propagating along the interface.

Equations (13)–(18) are the results of our analysis for the regular stripe-pattern region. The equations predict how the crack propagation velocity v, the distance between the stripes $L_{\rm c}$ and $L_{\rm n}$, and the frictional force $F_{\rm ave}$ depend on the experimental conditions such as pull velocity V, the shear modulus of the gel μ and the thickness of the gel-sheet H. Such an analysis has not been made in the previous works on the conventional Shallamach wave [8, 9], where one has to analyze the buckling of rubber sheet sliding on a substrate. The advantage of our gel-sheet system is that we can make a simple model for the detachment wave and can actually calculate the wave velocity and wavelength as a function of the pull velocity.

We then compare the theoretical prediction with the experimental results. Figure 7(a) shows the wave velocity v as a function of the pull velocity V. The wave velocity increases with the increase of the pull velocity (or the apparent sliding velocity) V, but they are not proportional to each other: the wave velocity v increases in proportion to $V^{0.75}$. In our experimental range, v is much larger than V, but they approach each other as the pull velocity increases. From the slope of the curve in figure 7(a), we determined the parameter α in equation (13). This gives $\alpha = 1/3$.

Figure 7(b) shows how the average length of the contact region $L_{\rm c}$ and that of the non-contact region $L_{\rm n}$ change with the pull velocity V. For small V, the contact region is much larger than the non-contact region. As the pull velocity V increases, the contact region decreases while the non-contact region increases. Accordingly, the fraction of the contact area decreases with the pull velocity. The experiments indicate that $L_{\rm c} \propto V^{-0.13}$ and $L_{\rm n} \propto V^{0.13}$. On the other hand, the theory predicts that the exponents are -0.125 (equation (15)) and 0.125 (equation (16)) if α is taken to be $1/3$. This is in good agreement with experiment.

Figure 7(c) shows how the average frictional force F depends on the pull velocity. The frictional force increases with the increase of the pull velocity, but the increase is weak: the slope of the curve is 0.15 experimentally. On the other hand, the theory (equation (17)) predicts that the slope is 0.125, which is again in good agreement with the experimental value.

The theory predicts how the parameters v, $L_{\rm c}$, $L_{\rm n}$ and F change when the shear modulus of the gel μ and the thickness of the gel-sheet H are changed. Preliminary experiments show that the theory is predicting the right direction of the change, but the detailed comparison will be done in a separate paper.

3.5. Collapse of the stripe patterns

We now discuss the mechanisms responsible for the collapse of the stripe patterns. When the stripe pattern is stable, the velocity of the crack opening edge $v_{\rm o}$ and the velocity of the crack closing edge $v_{\rm c}$ are equal to each other. As we decrease the pull velocity V, both $v_{\rm o}$ and $v_{\rm c}$ decrease. Since the crack opening is driven by the applied shear, $v_{\rm o}$ will approach zero as V goes to zero. On the other hand, $v_{\rm c}$ will have a lower limit, since the gel will spontaneously adhere to the substrate, or wet the substrate.

In order to see the wetting phenomena of the gel onto the substrate, we measured the spontaneous wetting velocity of the gel in a force-free state by the method shown in figure 8. A circular gel-sheet of radius $=$ 50 mm was hung vertically parallel to the glass plate with small separation ($\simeq$1 mm). The center of the gel-sheet was then gently brought into contact with the substrate and the velocity of the contact line was measured. This gave the 'wetting velocity' of the gel-sheet on the substrate $v_{\rm wet}$, which is $v_{\rm wet} = 4.0 \pm 1.5$ mm s^{-1}.

When the crack closing velocity $v_{\rm c}$ becomes less than $v_{\rm wet}$, the closing crack overtakes the opening ones, as is illustrated in figure 9, and the stripe pattern will become unstable. We therefore conjecture that the transition from the regular stripe pattern to the irregular bubble pattern takes place when the

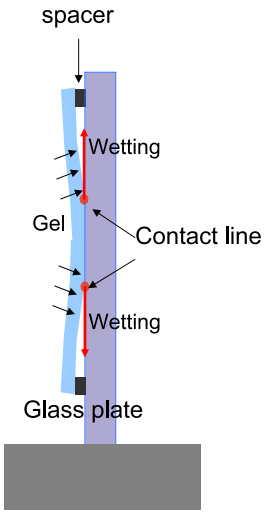

Figure 8. Schematic figure of the experimental apparatus for the measurement of the spontaneous wetting velocity.

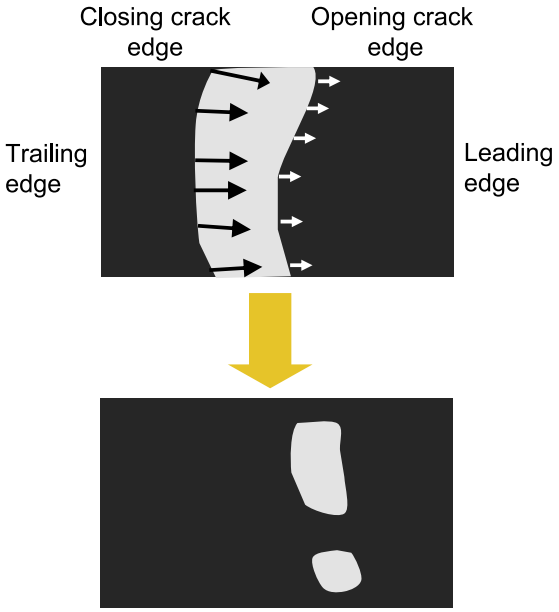

Figure 9. Schematic figure of collapse of stripe patterns at intermediate pull velocities.

crack propagation velocity v in the regular region becomes equal to the wetting velocity v_{wet}.

To check this conjecture, we extracted the curve of figure 7(a) to smaller velocity and estimated the pull velocity V^* which gives the crack propagation velocity equal to $v_{\mathrm{wet}} = 4.0\ \mathrm{mm\,s^{-1}}$. This gives $V^* \sim 50\ \mu\mathrm{m\,s^{-1}}$, which is in the middle of the transition region in figure 4, suggesting that our conjecture is reasonable.

4. Conclusion

We studied the motion of a soft and sticky gel-sheet sliding on a rigid substrate. We observed a regular stripe pattern at a large pull velocity and a bubble pattern at a small pull velocity. We found that the force drop obeys the power law statistics where the slope (b value) varies depending on the pull velocity. We proposed a simple model for the regular detachment wave at large pull velocity and predicted how the wave velocity, the contact and non-contact length and the average force depend on the pull velocity and other experimental parameters. The pull velocity dependence has been shown to agree well with experiments. We showed that the transition from the stripe pattern to the bubble pattern occurs when the crack opening velocity becomes comparable to the velocity of the spontaneous wetting of the gel-sheet on the substrate.

Acknowledgments

We thank D Rittel, H Nakanishi, Y Tanaka, M Sano, K Sekimoto, T Baumberger, O Ronsin, H Matsukawa, M Ohtsuki, T Hatano, T Yamaue and D Kaneko for many important comments and experimental support.

References

[1] Moore D F 1972 *The Friction and Lubrication of Elastomers* (Oxford: Pergamon)
[2] Persson B N J 2000 *Sliding Friction: Physical Principles and Applications* (New York: Springer)
[3] Grosch K A 1963 *Proc. R. Soc.* A **274** 21
[4] Vorvolakos K and Chaudhury M K 2003 *Langmuir* **19** 6778
[5] Persson B N J 2001 *Phys. Rev.* B **63** 104101
[6] Persson B N J and Volokitin A I 2006 *Eur. Phys. J.* E **21** 69
[7] Schallamach A 1971 *Wear* **17** 301
[8] Roberts A D and Jackson S A 1975 *Nature* **257** 119
[9] Roberts A D and Thomas A G 1975 *Wear* **33** 45
[10] Barquins M and Courtel R 1975 *Wear* **32** 133
[11] Barquins M and Roberts A D 1986 *J. Phys. D: Appl. Phys.* **19** 547
[12] Briggs A D and Briscoe B J 1976 *Nature* **262** 381
[13] Rand C J and Crosby A J 2006 *Appl. Phys. Lett.* **89** 261907
[14] Rubio M A and Galeano J 1994 *Phys. Rev.* E **50** 1000
[15] Baumberger T, Caroli C and Ronsin O 2002 *Phys. Rev. Lett.* **88** 75509
[16] Baumberger T, Caroli C and Ronsin O 2003 *Eur. Phys. J.* E **11** 85
[17] Chaudhury M K and Kim K H 2007 *Eur. Phys. J.* E **23** 175
[18] Maugis D 2000 *Adhesion and Rupture of Elastic Solids* (Berlin: Springer) (2002 (Cambridge: Cambridge University Press))
[19] Gutenberg B and Richter C F 1956 *Ann. Geophys.* **9** 1
[20] Gutenberg B and Richter C F 1954 *Seismicity of the Earth and Associated Phenomena* 2nd edn (Englewood Cliffs, NJ: Princeton University Press)
[21] Scholz C H 2002 *The Mechanics of Earthquakes and Faulting* 2nd edn (Cambridge: Cambridge University Press)
[22] Carlson J M and Langer J S 1989 *Phys. Rev. Lett.* **62** 2632
[23] Carlson J M, Langer J S and Shaw B E 1994 *Rev. Mod. Phys.* **66** 657
[24] Dalton F and Corcoran D 2001 *Phys. Rev.* E **63** 061312
[25] Bretz M, Zaretzki R, Field S B, Mitarai N and Nori F 2006 *Europhys. Lett.* **74** 1116
[26] Olami Z and Christensen K 1992 *Phys. Rev.* A **46** 1720
[27] Olami Z, Feder H J S and Christensen K 1992 *Phys. Rev. Lett.* **68** 1244
[28] Bak P and Tang C 1989 *J. Geophys. Res.* **94** 15635
[29] Persson B N J, Albohr O, Heinrich G and Ueba H 1999 *J. Phys.: Condens. Matter* **17** R1071
[30] Kendall K 1981 *Phil. Mag.* A **43** 713